

Laurenanes: Fenestranes with a Twist

Rex T. Weavers

Department of Chemistry, University of Otago, Box 56, Dunedin, New Zealand

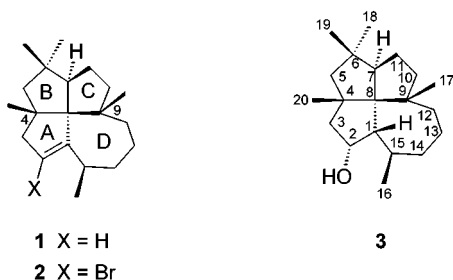
rweavers@alkali.otago.ac.nz

Received May 7, 2001

Four isomeric alcohols derived from the diterpene lauren-1-ene (**1**) have been examined by NMR methods (nuclear Overhauser enhancements, coupling constants, and variable-temperature studies) and by molecular mechanics using the MM3 force field to investigate a conformational twisting of the [5.5.5.7]fenestrane ring system. Results have been correlated with a concurrent study of remote functionalization reactions induced by iodobenzene diacetate/iodine under ultrasonic irradiation. Three of the laurenan-2-ols, **6**, **7**, and **8**, lead to the same tetrahydrofuran derivative, 2 β ,14 β -epoxylaurenane (**9**), and evidence for β -cleavage of the alkoxy radical intermediate is obtained through the isolation of a ring-cleavage product **11** with a rearranged carbon skeleton. The products from the remaining alcohol **3** demonstrate solution dynamics involving the conformational twisting of the laurenane skeleton.

Introduction

Despite the fact that it was first reported over 20 years ago,^{1,2} the naturally occurring diterpene, lauren-1-ene (**1**), remains the only known naturally occurring compound with an intact fenestrane ring system (rosettane).³ Furthermore, it has only been isolated from New Zealand plant sources, initially from *Dacrydium cupressinum* and, more recently, from some *Podocarpus* species.⁴



The structure of lauren-1-ene was determined by X-ray analysis of a bromo derivative **2**.² In the solid state, this compound existed in a conformation that avoided close interaction between the methyl groups at C-4 and C-9 by skewing the C-4 methyl toward the C-ring and the C-9 methyl toward the A-ring. This conformation, subsequently referred to as “skew 1”, is illustrated in Figure 1 for the basic laurenane skeleton, a substituted [5.5.5.7]-fenestrane. Indications that lauren-1-ene and its derivatives might adopt an alternative twist form were obtained

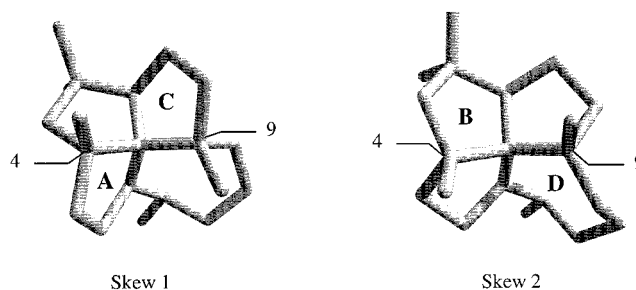


Figure 1. Skew conformations for laurenane, an *all-cis*-[5.5.5.7]fenestrane.

from analysis of the products of reaction of 1 β H-laurenan-2 α -ol (**3**) with lead tetraacetate and iodine.⁵ Cyclic ethers resulting from functionalization of both C-5 and C-7 were obtained. Examination of molecular models revealed that C-5 functionalization was compatible with a skew 1 conformation, but attack at C-7 required an alternative form where the C-4 and C-9 methyl groups had swapped orientations (skew 2, Figure 1). This represented a major conformational change affecting the whole molecule. Subsequently, the observation of line broadening in the ¹³C NMR spectrum of lauren-1(15),2-diene (**4**) has been interpreted in terms of a fluxional change involving skew 1 and skew 2 forms.⁶ Even more convincingly, the X-ray structure determination of a broken fenestrane derivative **5** revealed two molecules in the unit cell, one with a skew 1 conformation and the other with skew 2.⁷ The study described in this paper was designed to examine the solution behavior of compounds with the intact [5.5.5.7]-fenestrane skeleton to determine if there was any

(1) Corbett, R. E.; Lauren, D. R.; Weavers, R. T. *J. Chem. Soc., Perkin Trans. 1* **1979**, 1774–1790.

(2) Corbett, R. E.; Couldwell, C. M.; Lauren, D. R.; Weavers, R. T. *J. Chem. Soc., Perkin Trans. 1* **1979**, 1791–1794.

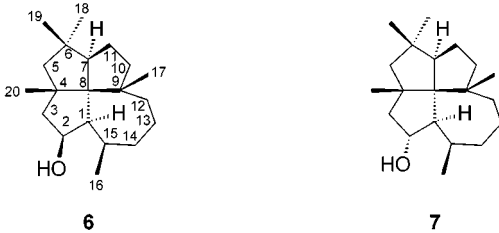
(3) Nickon, A.; Silversmith, E. F. *Organic Chemistry: The Name Game*; Pergamon Press: New York, 1987; pp 55–56.

(4) Clarke, D. B.; Hinkley, S. F. R.; Weavers, R. T. *Tetrahedron Lett.* **1997**, 38, 4297–4300.

(5) Nathu, N. K.; Weavers, R. T. *Aust. J. Chem.* **1980**, 33, 1589–1602.

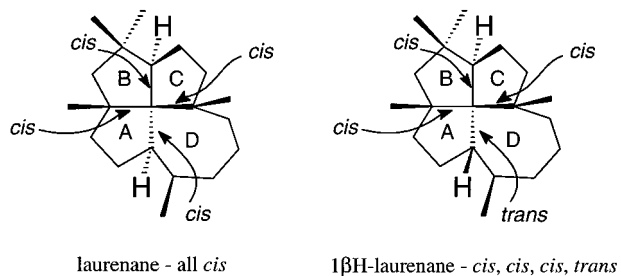
(6) Perry, N. B.; Weavers, R. T. *Aust. J. Chem.* **1988**, 41, 81–89.

(7) Hayman, A. R.; Simpson, J.; Weavers, R. T. *Aust. J. Chem.* **1988**, 41, 1571–1581.

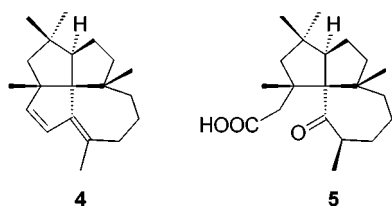
Table 1. Summary of Conformational Searching on Alcohols **3**, **6**, **7**, and **8**^a


form	population ^b (%)	$\cdot H_i$ /kcal mol ⁻¹	comments
laurenan-2 β -ol			
6-I	94.6	-81.0	skew 1
6-II	4.5	-79.2	skew 1
6-III	0.9	-78.2	skew 2
laurenan-2 α -ol			
7-I	86.8	-84.1	skew 1, like 6-I
7-II	13.2	-82.9	skew 1, C-O rotamer of 7-I, like 6-I
1 β H-laurenan-2 β -ol			
8-I	33.3	-82.0	skew 1
8-II	33.3	-82.0	skew 2
8-III	15.4	-80.5	skew 1
8-IV	5.4	-80.9	skew 1
8-V	4.5	-80.8	skew 1, C-O rotamer of 8-I
8-VI	3.5	-80.6	skew 1
8-VII	2.0	-79.3	skew 1, C-O rotamer of 8-III
8-VIII	1.4	-79.1	intermediary skew form
8-IX	0.7	-79.7	skew 1, C-O rotamer of 8-IV
8-X	0.5	-79.4	skew 1, C-O rotamer of 8-VI
1 β H-laurenan-2 α -ol			
3-I	33.6	-78.7	skew 1, like 8-III
3-II	31.0	-78.7	skew 2
3-III	28.3	-78.6	skew 2, like 8-II
3-IV	3.4	-77.4	skew 1, like 8-I
3-V	1.4	-76.8	skew 1, like 8-VI
3-VI	1.3	-76.8	skew 1
3-VII	0.5	-76.2	skew 2
3-VIII	0.5	-76.1	skew 2

^a MM3 force field. ^b Boltzmann distribution at 300 K.

**Figure 2.** Laurenane ring fusions.

significant distinction between those with the all *cis* geometry and those with a *cis, cis, cis, trans* arrangement.



Results and Discussion

all-cis-Fenestranes: Modeling and NMR Studies.

Laurenanes bearing a 1 α -hydrogen have a *cis* fusion between each pair of attached rings (Figure 2). This is

the geometry that has been encountered among most of the fenestranes synthesized to date.^{8,9}

Conformational searching of laurenan-2 β -ol (**6**), using the MM3 force field,¹⁰ generated three low energy conformations (Table 1, Figure 3). These same three structures resulted from two different search strategies. The two lowest energy forms, **6-I** and **6-II** (94.6% and 4.6% of the population, respectively), had a skew 1 geometry and essentially the same conformation of the seven-membered ring D. They differed primarily in the conformations of the five-membered rings A and B, with the lower energy structure having C-3 projecting upward and C-5 down and the other structure with these arrangements reversed. Given the flexibility of cyclopentane rings, it is likely that interconversion between these two forms would be facile. The remaining structure, **6-III** (0.9% of the population), had a skew 2 conformation. By contrast, the skew 1–skew 2 interconversion is likely to suffer a significant barrier through the interaction between the methyl groups at C-4 and C-9.

Disregarding rotamers about the C-2–O bond, modeling using the MMX force field¹¹ yielded five arrangements

(8) Thommen, M.; Keese, R. *Synlett* **1997**, 231–240.

(9) Bredenkötter, B.; Barth, D.; Kuck, D. *Chem. Commun.* **1999**, 847–848.

(10) (a) Allinger, N. L.; Yuh, Y. H.; Lii, J.-H. *J. Am. Chem. Soc.* **1989**, *111*, 8551–8566. (b) Lii, J.-H.; Allinger, N. L. *J. Am. Chem. Soc.* **1989**, *111*, 1, 8566–8575. (c) Lii, J.-H.; Allinger, N. L. *J. Am. Chem. Soc.* **1989**, *111*, 8576–8582.

(11) MMX, a modified MM2 force field, has been developed for PCModel²¹ by J. J. Gajewski and K. E. Gilbert.

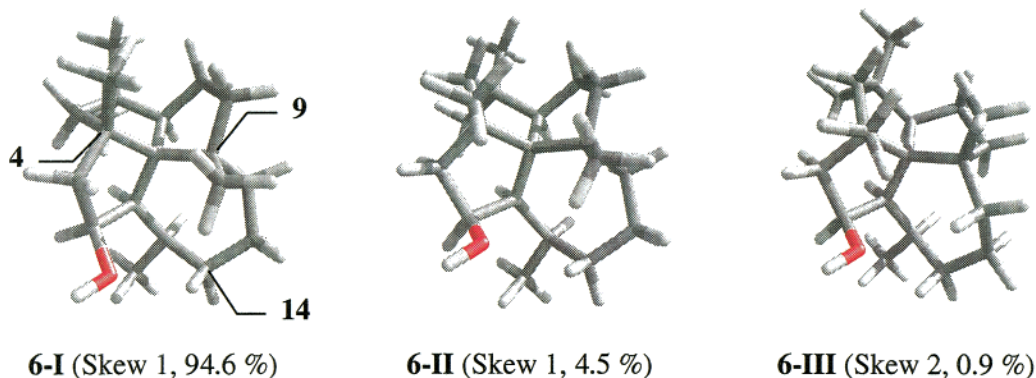


Figure 3. Calculated low energy conformations (MM3) for laurenan-2 β -ol (**6**).

Table 2. Observed and Calculated NMR Proton–Proton Coupling Constants for the Laurenan-2-ols^a

coupled pair	<i>J</i> /Hz			
	6 ^b	7 ^c	8 ^c	3 ^c
1,2	6 (6) {5}	9 (8)	10 (9)	6 (5)
1,15	3 (3) {3}	2 (2)	10 (10)	11 (11)
2,3 α	8 (9) {7}	3 (3)	7 (10)	0.5 (2)
2,3 β	3 (5) {4}	10 (10)	9 (7)	6 (7)
7,11 α	12 (10) {9}	12 (10)	8 (8)	10 (9)
7,11 β	5 (6) {7}	5 (6)	9 (9)	7 (6)
10 α ,11 α	8 (10) {8}	9 (10)	<i>d</i>	<i>d</i>
10 α ,11 β	2 (1) {6}	1 (1)	<i>d</i>	<i>d</i>
10 β ,11 α	11 (8) {6}	11 (8)	<i>d</i>	<i>d</i>
10 β ,11 β	10 (10) {7}	11 (10)	<i>d</i>	<i>d</i>
12 α ,13 α	<i>d</i>	5 (5)	<i>d</i>	<i>d</i>
12 α ,13 β	<i>d</i>	13 (12)	<i>d</i>	<i>d</i>
12 β ,13 α	3 (2) {7}	3 (2)	<i>d</i>	<i>d</i>
12 β ,13 β	6 (5) {3}	5 (5)	<i>d</i>	<i>d</i>
14 α ,15	<i>d</i>	<i>d</i>	5 (5)	6 (8)
14 β ,15	<i>d</i>	<i>d</i>	10 (10)	6 (8)

^a Calculated *J* values are weighted averaged values determined according to the Boltzmann distributions of the structures produced by conformational searching. ^b J_{obs} (J_{calcMM3}) { J_{calcMM3} }. ^c J_{obs} (J_{calcMM3}). ^d Coupling constants not measured due to peak overlaps

of the carbon skeleton. The lowest energy form was essentially the same as **6-I**, but in this case accounted for only 43.2% of the total population. The major difference here was the large contribution of the skew 2 form (41.3%).

Vicinal proton–proton coupling constants were calculated corresponding to signals that could be readily analyzed from the ¹H NMR spectrum (Table 2). Those based on the Boltzmann distributions of the structures from the MM3 modeling matched the observed values significantly better (± 2 Hz) than those derived from the MMX calculations (± 5 Hz). This suggests that the MMX calculation may overemphasize the contribution of the skew 2 conformation.

NOE experiments also support this conclusion (Table 3). When interproton distances were calculated for the low energy structure from the MM3 analysis, **6-I**, it was found that all observed NOE correlations corresponded to distances of less than 3.1 Å (this distance was used as a yardstick for interpreting the NOE results for the other laurenan-2-ol isomers). Most significantly, the observed interactions between H-20 and the 10 β and 11 β protons require a skew 1 conformation (Figure 3), as do interactions between the 3 β proton and H-17. No enhancements or correlations indicative of a skew 2 form, such as H-17 with H-5 β , or H-20 with any of H-12 β , H-13 β and H-14 β , were obtained.

Table 3. Key NOE Correlations Involving Bridgehead Groups for the Laurenan-2-ols

bridge-head group	NOE ^a			
	6	7	8	3
H-1	7	7	12 β ,14 β ,17	12,13,14 β ,17
4-Me (H-20)	10 β ,11 β ,17	10 β ,11 β ,17	10,11,17	10 β ,11,12,17
H-7	1,12 α ,15	1,12 α ,15	2,13,15	12,14 α ,15
9-Me (H-17)	3 β ,13 β ,14 β ,20	3 β ,13 β ,14 β ,20	1,3 β ,12 β ,20	1,3 β ,5 β ,12,13,20

^a Nuclear Overhauser enhancements involving the specified proton were determined from NOESY and/or 1D NOE experiments.

A number of correlations support a ring D conformation like that of **6-I** (Figure 3). The fact that C-13 and C-14 lie above the mean plane of this ring is supported by enhancements observed between H-17 and both H-13 β and H-14 β . C-15 projects down as shown by NOE involving H-15 and H-7. Likewise, C-12 lies toward the α -side of the ring as shown by reciprocal enhancements observed between H-7 and H-12 α . The fact that H-10 β projects toward H-20 places H-10 α in a periplanar arrangement with H-12 β . This accounts for the large chemical shift difference found for the two H-12 protons. H-12 α resonates at δ 2.00 while the H-12 β signal appears at δ 1.02. Likewise, the H-10 α and H-10 β signals appear at δ 1.29 and 1.93, respectively. Subsequent results show that these large chemical shift differences are good indicators for the dominance of a skew 1 conformation. As the NMR results showed no evidence for a significant contribution from a skew 2 conformation, the MM3 force field was used for all subsequent modeling.

With laurenan-2 α -ol **7**, conformational searching by two different search strategies yielded the same two low energy conformations (Table 1). These two structures differed significantly only in the rotation about the C-2–O bond and had a conformation of the carbon framework closely matching that of **6-I** (Figure 3).

Calculated coupling constants again showed good correlation with observed values (Table 2), the largest discrepancy being for $J_{10\beta,11\alpha}$ where a deviation of 3 Hz was noted. Given that the MM3 lowest energy conformations for **6** and **7** had virtually superimposable carbon frameworks, it was not surprising that the observed coupling constants for the two epimers matched very closely except for those involving the point of difference, C-2.

Further support for the proposed conformation came from NOE experiments (Table 3). All pairs of protons for which NOE was observed again lay within inter-nuclear

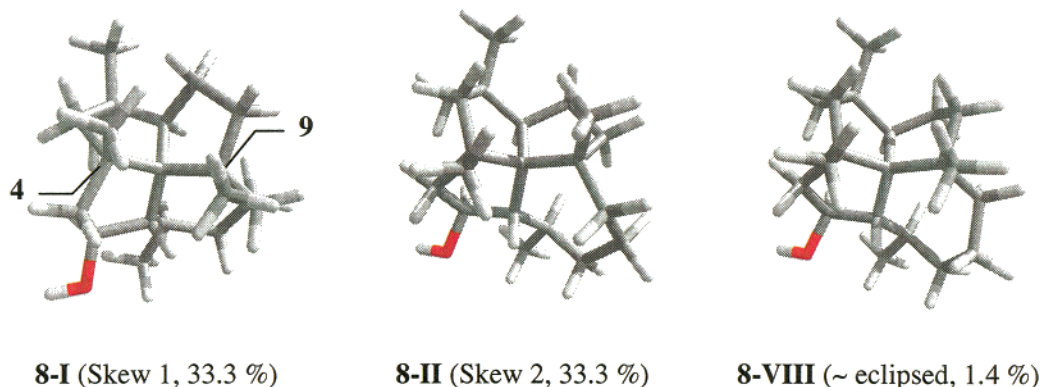
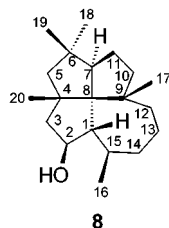


Figure 4. Two lowest energy conformers calculated (MM3) for $1\beta H$ -laurenan- 2β -ol (**8**) along with the almost eclipsing skew form.

distances of 3.1 Å in the calculated lowest energy structure. As in laurenan- 2β -ol, NOE observed for H-20 and H-17 require a skew 1 conformation and there is no evidence for a skew 2 form. Likewise, support for the proposed ring D conformation comes from enhancements observed between H-17 and both H- 13β and H- 14β and between H-7 and both H- 12α and H-15. Large chemical shift differences between the two H-12 protons (H- 12α δ 2.04; H- 12β δ 0.94) and between those at C-10 (H- 10α δ 1.14; H- 10β δ 1.96) were again noted.

cis, cis, cis, trans-Fenestranes: Modeling and NMR Studies. Introduction of a β -hydrogen at C-1 creates a trans A/D ring junction (Figure 2). Conformational searching of $1\beta H$ -laurenan- 2β -ol (**8**), using the MM3 force field, generated 10 conformations within a 3 kcal mol⁻¹ energy window (Table 1). Some of these differed only in rotation about the C-2–O bond, and there proved to be six distinct arrangements of the carbon framework. The lowest energy form **8-I** was again of the skew 1 type (Figure 4). When the C–O bond rotamer, **8-V**, was included, this arrangement of the carbon framework accounted for 37.8% of the population. Almost as significant was a form with a skew 2 skeleton, **8-II** (33.3%). Both **8-I** and **8-II** had similar conformations for the seven-membered ring D where C-12 and C-14 projected up and C-13 down. Three other arrangements of the carbon skeleton (**8-III/8-VII**, 17.4%; **8-IV/8-IX**, 6.1% and **8-VI/8-X**, 4.0%) had skew 1 structures with different ring D conformations. A particularly interesting form, **8-VIII** (1.4%), had the C-4 and C-9 methyl groups at virtually their closest approach with a C-20–C-4–C-9–C-17 angle of -6.1° (Figure 4). Although this must represent something close to the structure of the highest energy form to be encountered during the twisting process, it is a genuine local minimum under MM3.



¹H NMR spectra in either CDCl₃ or C₆D₆ were characterized by peak overlaps, and only a limited number of vicinal proton coupling constants were determined (Table 2). It is noteworthy that there was little, if any,

difference in chemical shift for each of the methylene pairs at C-10, C-11, and C-13. Where coupling constants were obtained, the values were within 3 Hz of those calculated from the Boltzmann distribution of the MM3 structures.

Unlike the situation with laurenan- 2β -ol (**6**) and laurenan- 2α -ol (**7**), not all pairs of protons that showed NOE interactions had internuclear distances of 3.1 Å or less in the skew 1 structure **8-I** (Figure 4). Exceptions were the pairs H-1/H- 3β , H-2/H- 5β , H-2/H-7, H- 3α /H- 5β , H- 3α /H-18, H- 5α /H-19, and H- 5α /H-20. In the skew 2 form **8-II**, even more pairs of protons yielding NOE were calculated to be further than 3.1 Å apart. However, almost all of the exceptions for the skew 1 structure had shorter than 3.1 Å contacts in the skew 2 form. H- 5β displayed NOE with both H-2 and H- 3α , but was calculated to be appreciably distant from both in either skew form. As similar signal amplifications were always observed for both the 5α and 5β protons in the 1D NOE experiments, these unexpected enhancements may be the result of a relay effect through the 5α -proton.

Observed interactions (Table 3) between H-20 and protons at C-10 and C-11, and between H- 3β and H-17, require a skew 1 conformation. The enhancement of the H-7 signal upon irradiation of H-2 and its reciprocal are consistent with some contribution from a skew 2 form.

Forms **8-I** and **8-II** have similar ring D conformations where both the 12β and 14β -protons project toward H-1 (Figure 4). NOE enhancements corresponding to both of these interactions were obtained. Interactions between the 7α -proton and one of the C-13 protons add further support to a significant contribution from such a seven-membered ring conformation.

The two conformations described here are very different from those calculated for compounds **6** and **7**. This is supported by substantial differences in the chemical shifts of some of the protons. In particular, the H-12 signals of **8** resonate at very similar frequencies (δ 1.44, 1.50) in contrast to the very large chemical shift difference noted in the $1\alpha H$ -series. Coupling constants are also significantly different (Table 2). NOE results suggest that a single conformation does not adequately describe the system and both NOE and coupling constant data are reasonably consistent with the MM3 based prediction of major Skew 1 and Skew 2 forms, each with a similar ring D conformation. In accordance with this picture of a dynamic system, there is significant line broadening in the ¹³C NMR spectrum of **8** at -40°C for C-1, C-3, C-13,

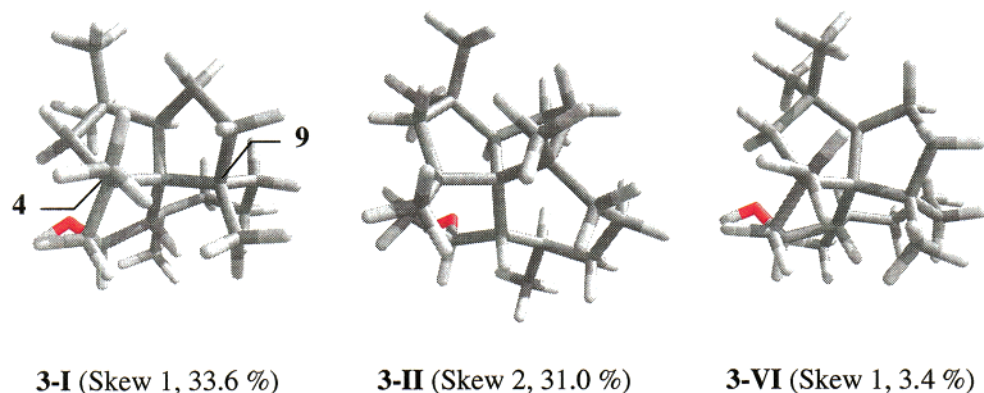


Figure 5. Selected conformations calculated (MM3) for $1\beta H$ -laurenan- 2α -ol (**3**).

C-14, C-15, and C-17. By contrast, sharp lines were observed for all ^{13}C NMR signals for the $1\alpha H$ -derivatives, **6** and **7**, over the temperature range -40 to $+45$ °C.

Conformational searching of $1\beta H$ -laurenan- 2α -ol (**3**) yielded eight low energy conformations, all with significant differences in the arrangement of the carbon skeleton (Table 1). Four of these were of the skew 1 type, and four possessed skew 2. The lowest energy conformation **3-I** (Figure 5, 33.6% of the population) was a skew 1 form corresponding to a higher energy form of the 2β -epimer, **8-III**. Similar in energy was a skew 2 form, **3-II** (31.0%), that was not represented in the structure set derived for **8**. The next two conformations found were a skew 2 form, **3-III** (28.3%), and a skew 1 form, **3-IV** (3.4%). These two structures matched closely the lowest energy skew 2 and skew 1 geometries calculated for **8**. It is noteworthy that, unlike the other three isomeric alcohols, the predicted population of skew 2 forms for this compound exceeds 50% (skew 1—39.7%; skew 2—60.3%).

Again, ^1H NMR spectra were complicated by peak overlaps, and some methylene pairs (C-11, C-12, and C-13) resonated at almost the same frequency. Where coupling constants could be determined, the observed values were within 2 Hz of those calculated from the modeled structures (Table 2). The predicted $J_{14\alpha,15}$ value for the lowest energy conformation **3-I** (1 Hz) is quite small, while that for all other conformations except the penultimate one is large (11–12 Hz). The fact that the observed value (6 Hz) is less than the predicted weighted averaged value (8 Hz) may reflect a greater contribution from the lowest energy skew 1 form than predicted.

As with the 2β -epimer, **8**, no one conformation had proton–proton separations less than 3.1 Å for all pairs of nuclei that displayed NOE. Interactions that did not seem compatible with the lowest energy skew 1 conformation **3-I** were H-1/H- 12β and H-20; H- 3α /H-18; H- 5β /H-17; H- 12β /H-20 and H- 13α /H-15. However, in the lowest energy skew 2 form **3-II**, these proton systems were all in close proximity while some other interacting nuclei were well separated. Once again, the NOE interactions could be accommodated by a dynamic system. Skew 1 form **3-I** (Figure 5) accounts for observed interactions (Table 3) between H-20 and protons at C-10 and C-11, and those between H-17 and both H-1 and H- 3β . However, the enhancement of the H- 5β signal upon irradiation of H-17, and correlations observed between H-20 and H-12, definitely require a contribution from a Skew 2 form. The conformational equilibrium proposed here differs significantly from that proposed for **8** and

this is supported by appreciable differences in the coupling constants found for these two epimers (Table 2). As for **8**, significant line broadening was found in the ^{13}C NMR spectrum at -40 °C. Peaks affected were widely distributed about the molecule (carbons 1, 3, 10, 12, 13, 14, 16, 17, 19, and 20) as expected for a skew 1/skew 2 type of interconversion.

The signal broadening in the ^{13}C NMR spectra of the $1\beta H$ -derivatives **3** and **8** at lower temperature is consistent with a slowing of the skew interchange. Modeling of **8** produced a form, **8-VIII**, with an intermediary skew structure that must have very similar geometry to the highest energy form on the skew exchange path. The fact that **8-VIII** and the lowest energy conformer, **8-I**, differ in heat of formation by only 2.9 kcal mol $^{-1}$ is consistent with a low barrier to interconversion. The lack of signal broadening found in the $1\alpha H$ -laurenan derivatives **6** and **7**, over the temperature range -40 to $+45$ °C, is compatible with either a lack of significant skewing motion, or with a very rapid process. However, the fact that skew 2 forms feature so little in the predicted populations from MM3 modeling for these compounds suggests strongly that the former option is true.

Remote Functionalization. Generation of an alkoxy radical provides a well explored avenue for the functionalization of a molecule at a position remote from a hydroxyl group.¹² The prerequisite is a hydrogen-bearing atom located at position 4 relative to the oxygenated center, as the hydrogen abstraction generally proceeds through a six-membered transition state. It has been established that there is a preference for attack at more highly substituted carbon atoms.¹³

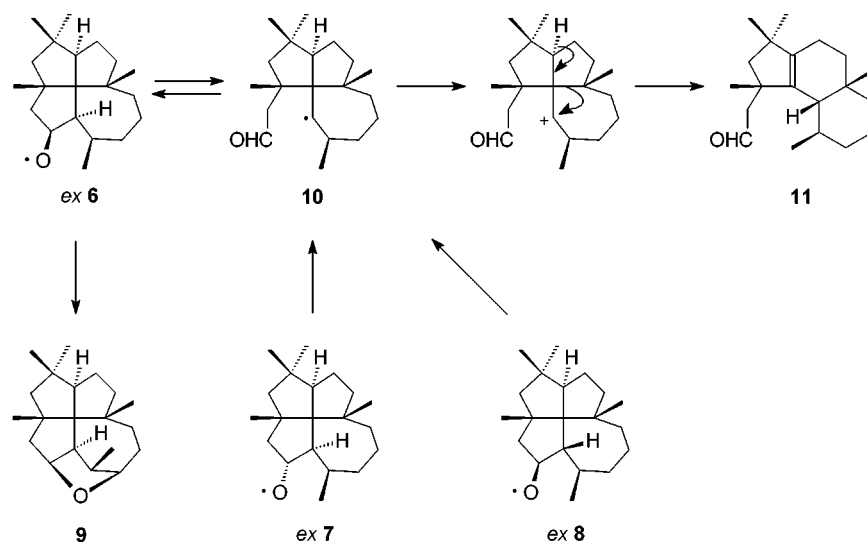
Remote functionalization of alcohols **6**, **7** and **8** was examined in this study, making use of the recently described iodine/iodobenzene diacetate/ultrasound system.¹⁴ As had been noted previously in reactions with iodine/lead tetraacetate,⁵ all three compounds gave the same tetrahydrofuran derivative **9**. Yields from the two reaction systems were not markedly different. It appears that the initially formed alkoxy radical undergoes cleavage of the C-1 to C-2 bond to produce a tricyclic aldehyde intermediate **10** with a radical center at C-1. 5-*Exo-trig* re-closure of this species provides a mechanism for

(12) For a recent review, see: Majetich, G.; Wheless, K. *Tetrahedron* **1995**, *51*, 7095–7129.

(13) Heusler, K.; Kalvoda, J. *Angew. Chem., Int. Ed. Engl.* **1964**, *3*, 525–538.

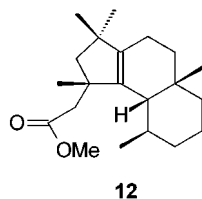
(14) Costa, S. C. P.; Moreno, M. J. S. M.; Sá e Melo, M. L.; Campos Neves, A. S. *Tetrahedron Lett.* **1999**, *40*, 8711–8714.

Scheme 1



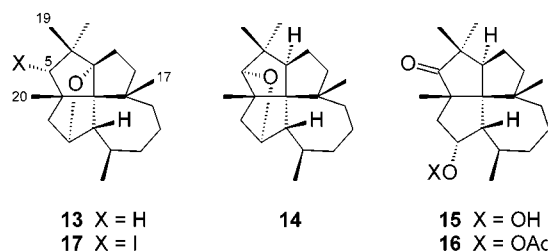
changing the stereochemistry at either or both of C-1 and C-2 (Scheme 1).

The iodobenzene diacetate/iodine treatments of **6–8** also yielded a common byproduct, a new compound, tricyclic aldehyde **11**. This structure was deduced from various NMR correlation experiments, and there was excellent correlation between the derived ^{13}C NMR data and those reported for the related methyl ester **12**.¹⁵ Formation of **11** provides strong support for the proposed radical cleavage mechanism (Scheme 1). Generation of cationic species at C-1 in ring A seco laurenanes is known to initiate rapid alkyl migration reactions.¹⁵ These convert the constrained central C-8 atom into a less congested planar environment. Thus, it would appear that the proposed C-1 radical intermediate **11** is formally oxidized to a cation that subsequently rearranges (Scheme 1). Such a single-electron-transfer process has been employed in the formation of *N*-acyliminium ions, where appropriate carbon-centered radicals were generated through decarboxylation of carboxylic acids by iodine/iodobenzene diacetate treatment.¹⁶



Reaction of $1\beta\text{H}$ -laurenan- 2α -ol (**3**) with iodobenzene diacetate/iodine in the current investigation led to functionalization at both C-5 and C-7 as had been found with lead tetraacetate/iodine.⁵ The previously reported products of mono-functionalization, $2\alpha,7\alpha$ -epoxy- $1\beta\text{H}$ -laurenane (**13**) and $2\alpha,5\alpha$ -epoxy- $1\beta\text{H}$ -laurenane (**14**), were obtained, along with two products resulting from difunctionalization. Two successive attacks at C-5 led to ketol, (**15**) which showed ill-defined NMR spectra, presumably as a result of contributions from an internal hemiacetal form. This compound was fully characterized

as its acetate (**16**). Attack at C-5 followed by attack at C-7 resulted in a new compound, 5α -iodo- $2\alpha,7\alpha$ -epoxy- $1\beta\text{H}$ -laurenane (**17**). The C-5 stereochemistry of **17** followed from NOE experiments where irradiation of H-5 led to enhancements of the H-17, H-19, and H-20 signals.



Formation of compound **14** clearly requires a skew 1 conformation, while a skew 2 form is necessary to yield **13**. Compound **17** derives from initial attack at C-5 in a skew 1 conformation, but requires subsequent conformational change to a skew 2 form to allow ether ring formation to C-7. The 5α -orientation of the iodo group is not conducive to the cyclization required for the formation of **14** or to further attack at C-5 leading to **15**. Unlike the other three alcohols, reaction of **3** led to the isolation of no products resulting from β -cleavage of the initially formed alkoxy radical.

The results of these experiments can now be rationalized to some extent in terms of the detailed understanding of the conformations of these systems gained through molecular modeling and NMR study. In the early literature it was proposed that functionalization of a steroidal methyl group was only feasible if the distance between the oxygen radical center and the methyl carbon was less than 2.8 \AA .¹³ However, this estimate was made on the basis of measurements performed with a ruler on Dreiding models. A more recent MM2 study extended this distance to about 3.05 \AA .¹⁷ The early literature proposed that reaction proceeded best if a chair transition state could be attained,¹³ but it is currently accepted that hydrogen abstraction ideally proceeds through a transition state with a linear arrangement of the oxygen, the

(15) Hanton, L. R.; Lorimer, S. D.; Weavers, R. T. *Aust. J. Chem.* **1987**, *40*, 1795–1812.

(16) Boto, A.; Hernández, R.; Suárez, E. *J. Org. Chem.* **2000**, *65*, 4930–4937.

(17) Burke, S. D.; Silks, L. A.; Strickland, S. M. S. *Tetrahedron Lett.* **1988**, *29*, 2761–2764.

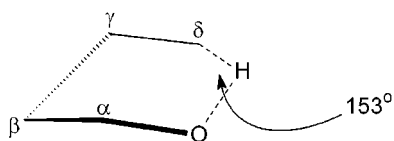


Figure 6. Proposed transition state for intramolecular hydrogen atom abstraction by an alkoxy radical.

Table 4. Ranges of C–O Distances Calculated for Modeled Conformations, Corresponding to Possible Sites of Remote Functionalization^a

compd ^b	O–C5	O–C7	O–C14	O–C16	O–C20
6 (3)	4.48–4.50	4.54–4.85	2.96–3.09	3.28–3.78	3.09–4.64
7 (2)	3.67–3.69	4.72–4.81	3.95–4.02	3.05–3.06	4.81–4.86
8 (10)	4.33–4.82	4.46–4.98	4.10–4.58	2.89–3.03	4.37–4.88
3 skew 1 (4)	2.92–2.99	3.79–3.92	4.40–4.48	2.99–3.26	4.48–4.51
3 skew 2 (4)	3.97–4.34	3.00–3.28	4.26–4.49	2.91–3.17	4.62–4.64

^a Distances in Å. Entries in **bold italics** correspond to sites where functionalization has been found experimentally. ^b Number of conformations in parentheses.

migrating hydrogen and the carbon center. In an intramolecular reaction, this arrangement is compromised by the strain developing in the cyclic array and ab initio studies have led to the proposal of a transition state (Figure 6) where the O–H–C_δ angle is 153° and the five heavy atoms make up an envelope conformation.¹⁸ The migrating hydrogen is calculated to lie almost in the O–C_α–C_γ–C_δ plane, but slightly to the side opposite C_β.

Positions 5, 7, 14, 16, and 20 of the laurenan-2-ols are the centers corresponding to C_δ in Figure 4; those potentially available for remote functionalization. Examination of calculated C–O distances for each of the modeled conformations (Table 4) shows that attack at C-20 is unlikely in all cases, except perhaps for the skew 2 form **6-III** where the separation is measured as 3.09 Å. Alcohol **3** is the only isomer where the C–O distance seems to favor attack at C-5 or C-7. The former option requires a skew 1 conformation and the latter a skew 2. Attack at C-14 only seems feasible for compound **6**, while attack at C-16 appears to be possible in all isomers except **6**. However, experimental results reveal functionalization only at C-14 in **6** and at C-5 and C-7 in **3**. In each of these instances C–O distances in some accessible conformations are calculated to be less than 3.1 Å, sufficiently short to permit hydrogen abstraction.¹⁷ The lack of observed attack at C-16 may simply reflect the reduced reactivity of a methyl grouping,¹³ but more probably relates to the fact that this methyl is probably too conformationally mobile to be held in a rigid transition state.

Table 5 shows some additional data calculated for instances where the C–O distance is less than 3.1 Å. It can be seen that, where reaction does take place, there is at least one conformer where the calculated O–H distance is less than 2.3 Å. Perhaps more significantly, these occurrences are marked by at least one conformation where the O–H–C_δ angle has widened to more than 125°. Although this value is well short of the optimum value of 153° calculated by ab initio methods for the hydrogen abstraction transition state,¹⁸ the geometry of the parent alcohol is perturbed to an appreciable extent in this direction.

Table 5. Key Angles and Distances Calculated for Cases with C–O Separation <3.1 Å^a

potential attack site ^b	O–H/Å	O–C _α –C _γ –C _δ /deg	O–H–C _δ /deg
C-14 in 6	2.17–2.33	–23.7–5.0	120.0–127.9
C-20 in 6-III	2.50	–20.3	111.4
C-16 in 7	2.54–2.58	–15.0 to –8.6	104.5–107.0
C-16 in 8	2.45–2.73	18.5–46.2	93.4–106.4
C-16 in 3	2.31–2.38	–66.7 to –76.5	111.7–115.6
C-5 in 3 (skew 1)	2.12–2.38	–2.2–0.2	111.6–128.2
C-7 in 3 (skew 2)	2.22–2.36	11.6–12.6	116.4–128.6

^a Distances and angles are measured to the closest hydrogen in the minimized structure. ^b Entries in **bold italics** correspond to experimentally observed functionalizations.

The optimum conformation for C-14 functionalization in **6** would appear to be **6-II** (Figure 3) where the O–H distance is calculated as 2.28 Å and the O–H–C_δ angle is 127.9°. In this conformation O, C_α, C_γ, and C_δ are almost planar (O–C_α–C_γ–C_δ = –5.5°). The hydrogen to be abstracted lies almost in this plane, similar to the transition state in the ab initio study (Figure 6). Likewise, for C-5 attack in **3**, the optimum conformation seems to be **3-VI** (Figure 5) where the O–H distance is 2.12 Å, the O–H–C_δ angle is 128.2, and the O–C_α–C_γ–C_δ torsion angle is 0.2°. Again, the hydrogen lies approximately in the plane of the O, C_α, C_γ, and C_δ atoms. For C-7 attack in **3**, the optimum conformation is probably the lowest energy, skew 2 form, **3-II** (Figure 5), with an O–H distance of 2.22 Å and an O–H–C_δ angle of 128.6°. In this case, there is a little more distortion from planarity with the O–C_α–C_γ–C_δ angle at 12.6°, but again the hydrogen to be abstracted lies approximately in the mean plane of this subunit. C-14 attack in **6** suffers from competitive β-cleavage of the alkoxy radical. C-5 and C-7 attack in **3** do not. This is in accordance with the longer O–H contact and the narrower O–H–C_δ angle in the former case.

Conclusions

This study has shown that the MM3 force field and conformational searching applied to a relatively complex dynamic system, within a readily available and simple to use molecular modeling package, leads to predictions which correlate well with observed solution behaviors. These include proton–proton couplings and proton NOE interactions from NMR studies, and the analysis of remote functionalization reactions. MM3 gives a better match with experimental results than MMX, a modified MM2 force field. Similar results have been noted in modeling studies on the caryophyllene system.¹⁹

Results obtained in this study suggest that the *all-cis*-[5.5.5.7]fenestrane system of the laurenanes exists predominantly in the skew 1 conformation where the C-4 methyl group projects toward ring C. In the *cis,cis,cis*, *trans* compounds, the 1β*H*-laurenanes, the solution equilibria are more complex, involving skew 1 forms with the C-4 methyl group projecting toward ring C and skew 2 forms where this group points over ring D.

Iodine/iodobenzene diacetate remote functionalization reactions carried out on the four isomeric laurenan-2-ols under ultrasonication have produced the same tetrahydrofuran derivatives obtained in an earlier study

(18) Dorigo, A. E.; Houk, K. N. *J. Am. Chem. Soc.* **1987**, *109*, 2195–2197.

(19) Huebner, M.; Rissom, B.; Fitjer, L. *Helv. Chim. Acta* **1997**, *80*, 1972–1982.

with iodine/lead tetraacetate.⁵ However, two significant new byproducts have been isolated. In each case, reaction proceeds by formation of an alkoxy radical. This may functionalize an appropriate center if the geometry is favorable, as is observed in the case of laurenan-2 β -ol (**6**), which is converted to 2 β ,14 β -epoxylaurenane (**9**), and in the case of 1 β H-laurenan-2 α -ol (**3**), which yields both 2 α ,7 α -epoxy-1 β H-laurenane (**13**) and 2 α ,5 α -epoxy-1 β H-laurenane (**14**).

If hydrogen abstraction is significantly slow, as is obviously the case with laurenan-2 β -ol (**6**), laurenan-2 α -ol (**7**), and 1 β H-laurenan-2 β -ol (**8**), a β -cleavage process becomes competitive. The resulting intermediate radical is trapped to some extent as the rearranged aldehyde **11**, but can recombine with the aldehyde grouping to provide a pathway whereby the stereochemistry at carbons 1 and 2 may be altered (Scheme 1). It is quite likely that this opening and closing is taking place reversibly with radicals of various stereochemistries being formed. Nonetheless, reversion to an alkoxy radical with a 1 β -hydrogen and a 2 α -oxygen definitely does not occur to any significant extent, as reaction of **6**, **7** or **8** results in no observable functionalization at C-5 or C-7, the result found for 1 β H-laurenan-2 α -ol (**3**). The lack of β -cleavage products from the reaction of **3** indicates that it undergoes particularly fast hydrogen atom abstraction.

Analysis of the products from the remote functionalization of **3** leaves no doubt that skew 1 and skew 2 forms of the fenestrane skeleton do exist in solution. Formation of iodo ether **17** demonstrates that the skew interchange must be reasonably fast to allow one instance of functionalization in one twist conformation, followed by a repeat in the other.

This study has demonstrated that examination of minimized structures from molecular mechanics provides a valuable tool for prediction of the outcomes of remote functionalization reactions. In addition to examining C–O distances, it is also useful to measure O–H separations and to examine the angle between the oxygen atom, the migrating hydrogen and the attached carbon.

Experimental Section

General Methods. All solvents were distilled prior to use. Column chromatography was carried out on silica gel 60 (0.063–0.2 mm). Preparative TLC was performed on Merck silica coated glass plates with a layer thickness of 0.5 mm.

NMR Studies. NMR spectra were recorded on ca. 0.075 M CDCl₃ solutions at 500 MHz for ¹H and 125.7 MHz for ¹³C and were referenced to the CHCl₃ peak (δ 7.26) for ¹H and to the center line of the CDCl₃ signal (δ 77.08) for ¹³C. Spectra were assigned with the aid of double-quantum filtered COSY (¹H–¹H correlation), DEPT (number of H per C), HSQC (one-bond ¹H–¹³C correlation), and HMBC-CIGAR²⁰ (two- and three-bond ¹H–¹³C correlation) experiments. ¹H–¹H close approaches were determined with the aid of NOESY spectra (mixing time 0.8 s), and, in some cases, by using one-dimensional NOE experiments. Where appropriate, single frequency ¹H-decoupling experiments were used to simplify proton multiplets. Data obtained for the four alcohols used in this study are listed below.

IR Spectra. IR spectra were recorded on an FT IR instrument as films (liquids) or as KBr disks (solids).

Molecular Mechanics Calculations. These were performed with the aid of PCModel version 7.²¹ Conformational searches used either MM3¹⁰ or MMX¹¹ force fields, with the

mixed Monte Carlo coordinate movements/bond rotations strategy²² for the generation of initial structures. The default cutoff criteria were employed. Coupling constants were derived for each of the structures generated within a 3 kcal mol⁻¹ energy window, using the in-built modified Karplus calculation,²³ and Boltzmann averaged values were determined.

Laurenan-2-ol Isomers. 1 β H-Laurenan-2 α -ol (**3**) {[1*R*-(1 α ,2 $\alpha\beta$,4 $\alpha\alpha$,6 $\alpha\beta$,10 β ,10 $\alpha\beta$,10*bR*^{*})]-tetradecahydro-2 α ,4,4,6 α ,10-pentamethylpentaleno[1,6-*cd*]azulen-1-ol, CN 72075-55-9}, laurenan-2 β -ol (**6**) {[1*S*-(1 α ,2 $\alpha\alpha$,4 $\alpha\beta$,6 $\alpha\alpha$,10 α ,10 $\alpha\beta$,10*bS*^{*})]-tetradecahydro-2 α ,4,4,6 α ,10-pentamethylpentaleno[1,6-*cd*]azulen-1-ol, CN 72075-57-1}, laurenan-2 α -ol (**7**) {[1*R*-(1 α ,2 $\alpha\beta$,4 $\alpha\alpha$,6 $\alpha\beta$,10 β ,10 $\alpha\alpha$,10*bR*^{*})]-tetradecahydro-2 α ,4,4,6 α ,10-pentamethylpentaleno[1,6-*cd*]azulen-1-ol, CN 72075-58-2} and 1 β H-laurenan-2 β -ol (**8**) {[1*S*-(1 α ,2 $\alpha\alpha$,4 $\alpha\beta$,6 $\alpha\alpha$,10 α ,10 $\alpha\alpha$,10*bS*^{*})]-tetradecahydro-2 α ,4,4,6 α ,10-pentamethylpentaleno[1,6-*cd*]azulen-1-ol, CN 72062-09-0} were prepared as in ref 1.

Remote Functionalization Reactions. A solution of the alcohol (0.100 g, 0.344 mmol) in cyclohexane (2.5 mL) was agitated with iodobenzene diacetate (0.150 g, 0.466 mmol) and iodine (0.100 g, 0.390 mmol) in an ultrasonic cleaning bath at 40–45 °C for 15 min. Powdered Na₂S₂O₃·5H₂O (0.5 g) and water (5 drops) were added, and the mixture was shaken until the iodine color dissipated. Treatment with anhydrous MgSO₄ (8 g) followed by filtration and evaporation gave a crude mixture that was chromatographed on a column of silica gel (10 g). Initial elution with cyclohexane (20 mL) removed iodobenzene.

IBDA/I₂ on Laurenan-2 β -ol (6**).** Elution with chloroform gave [1*S*-(1 α ,5 $\alpha\beta$,9 β ,9 $\alpha\beta$)]-2,3,4,5,5 α ,6,7,8,9,9 α -decahydro-1,3,3,5 α ,9-pentamethyl-1*H*-benz[*e*]inden-1-ol (**11**) (0.016 g, 16%) followed by 2 β ,14 β -epoxylaurenane (**9**)⁵ {[1*R*-(1 α ,2 $\alpha\beta$,3 α ,4 $\alpha\alpha$,6 $\alpha\beta$,10 β ,10 $\alpha\beta$,10*bR*^{*})]-tetradecahydro-2 α ,4,4,6 α ,10-pentamethyl-1,3-epoxypentaleno[1,6-*cd*]azulene, CN 76236-71-0} (0.070 g, 70%). Elution with ether gave a complex mixture (0.017 g). Compound **11**: IR (film) 2723, 1722 (–CHO) cm⁻¹; ¹H NMR (500 MHz, CDCl₃) δ 0.73 (d, *J* = 1 Hz, H-17, 3H), 0.83 (d, *J* = 7 Hz, H-16, 3H), 0.88 (m, H-10 β , 1H), 1.00 (m, H-14 β , 1H), 1.04 (s, H-18, 3H), 1.07 (s, H-19, 3H); 1.10 (d, *J* = 1 Hz, H-20, 3H), 1.26 (d, *J* = 7 Hz, H-1, 1H), 1.27 (m, H-12 α , 1H), 1.41 (m, H-15, 1H), 1.47 (m, H-13 β , 1H), 1.48 (m, H-12 β , 1H), 1.59 (m, H-13 α , 1H), 1.60 (m, H-14 α , 1H), 1.88 (s, H-5, 2H), 2.03 (m, H-11, 2H), 2.16 (dd, *J* = 9, 14 Hz, H-10 α , 1H), 2.42 (ddq, *J* = 2, 14, 1 Hz, H-3 α , 1H), 2.52 (dd, *J* = 4, 14 Hz, H-3 β , 1H), 9.83 (dd, *J* = 2, 4 Hz, H-2, 1H); ¹³C NMR (125.7 MHz, CDCl₃) δ 18.01 (C-11), 21.91 (C-13), 23.81 (C-16), 26.65 (C-19), 26.84 (C-10), 27.69 (C-20), 29.07 (C-17), 30.61 (C-18), 35.05 (C-9), 35.37 (C-15), 36.70 (C-14), 39.94 (C-12), 44.35 (C-6), 46.48 (C-4), 48.67 (C-1), 53.33 (C-5), 57.57 (C-3), 141.20 (C-7), 141.77 (C-8), 204.45 (C-2). A sample for microanalysis was prepared by micro-distillation at 105 °C/0.04 mmHg. Anal. Calcd for C₂₀H₃₂O: C, 83.27; H, 11.18. Found: C, 83.01; H, 11.15. Compound **9** was identical to an authentic sample (¹H and ¹³C NMR).⁵

IBDA/I₂ on Laurenan-2 α -ol (7**).** Elution with chloroform gave rearranged aldehyde **11** (0.034 g, 34%) followed by 2 β ,14 β -epoxylaurenane (**9**) (0.042 g, 42%). Elution with ether gave a complex mixture (0.022 g).

IBDA/I₂ on 1 β H-Laurenan-2 β -ol (8**).** Elution with chloroform gave rearranged aldehyde **11** (0.046 g, 46%) followed by 2 β ,14 β -epoxylaurenane (**9**) (0.042 g, 42%). Elution with ether gave a complex mixture (0.017 g).

IBDA/I₂ on 1 β H-Laurenan-2 α -ol (3**).** Elution with ether/hexanes (1:19) gave a mixture consisting mainly of **13** and **17** (0.040 g) followed by 2 α ,5 α -epoxy-1 β H-laurenane (**14**)⁵ {[1*R*-(1 α ,2 $\alpha\beta$,3 α ,4 $\alpha\alpha$,6 $\alpha\beta$,10 β ,10 $\alpha\beta$,10*bR*^{*})]-tetradecahydro-2 α ,4,4,6 α ,10-pentamethyl-1,3-epoxypentaleno[1,6-*cd*]azulene, CN 76236-71-0} (0.028 g, 28%). Elution with ether/hexanes (1:1)

(21) PCModel, version 7.0, Serena Software, Box 3076, Bloomington, IN 47402-3076.

(22) Saunders, M.; Houk, K. N.; Wu, Y.-D.; Still, W. C.; Lipton, M.; Chang, G.; Guida, W. *J. Am. Chem. Soc.* **1990**, *112*, 1419–1427.

(23) Haasnoot, C. A. G.; De Leeuw, F. A. A. M.; Altona, C. *Tetrahedron* **1980**, *36*, 2783–2792.

(20) Hadden, C. E.; Martin, G. E.; Krishnamurthy, V. V. *Magn. Reson. Chem.* **2000**, *38*, 143–147.

gave 2 α -hydroxy-1 β *H*-laurenan-5-one (**15**)⁵ {[1*R*-(1 α ,2 $\alpha\beta$,4 $\alpha\alpha$,6 $\alpha\beta$,10 β ,10 $\alpha\beta$,10 βR^*)]-dodecahydro-1-hydroxy-2 α ,4,4,6 α ,10-pentamethylpentaleno[1,6-*cd*]azulen-3(1*H*)-one, CN 76236-72-1} (0.022 g, 21%). Further chromatography of the mixture of **13** and **17** on silica gel (10 g), eluting with benzene, gave 5 α -iodo-2 α ,7 α -epoxy-1 β *H*-laurenane (**17**) {[1*R*-(1 α ,2 $\alpha\beta$,4 $\alpha\alpha$,5 α ,6 $\alpha\beta$,10 β ,10 $\alpha\beta$,10 βS^*)]-dodecahydro-5-iodo-2 α ,4,4,6 α ,10-pentamethyl-1*H*-1,4a-epoxypentaleno[1,6-*cd*]azulene} (0.021 g, 21%) followed by 2 α ,7 α -epoxy-1 β *H*-laurenane (**13**)⁵ {[1*R*-(1 α ,2 $\alpha\beta$,4 $\alpha\alpha$,6 $\alpha\beta$,10 β ,10 $\alpha\beta$,10 βS^*)]-dodecahydro-2 α ,4,4,6 α ,10-pentamethyl-1*H*-1,4a-epoxypentaleno[1,6-*cd*]azulene, CN 76236-77-6} (0.007 g, 7%). Compounds **13** and **14** were identical to authentic samples (¹H and ¹³C NMR).⁵ Compound **15** had IR (KBr) 3427 (OH), 1711 (C=O) cm⁻¹; MS 304 (M⁺), 234, 217, 147, and was characterized by conversion into its acetate **16** (vide infra). Compound **17**: IR (KBr) 1233, 1244, 1167, 1131, 1103, 1075, 1034, 1024, 1007, 989, 955, 923, 896, 866, 835, 777, 696 585 cm⁻¹; ¹H NMR (500 MHz, CDCl₃) δ 0.98 (d, *J* = 7 Hz, H-16, 3H), 1.06 (m, H-14 β , 1H), 1.14 (s, H-19, 3H), 1.18 (dm, *J* = 14 Hz, H-3 β , 1H), 1.22 (s, H-18, 3H), 1.23 (s, H-20, 3H), 1.26 (s, H-17, 3H), 1.49 (m, H-10 β , 1H), 1.49 (m, H-12 α , 1H), 1.62 (m, H-13 β , 1H), 1.66 (m, H-14 α , 1H), 1.70 (m, H-12 β , 1H), 1.72 (d, *J* = 9 Hz, H-1, 1H), 1.72 (m, H-13 α , 1H), 1.73 (m, H-11 β , 1H), 1.80 (m, H-15, 1H), 2.04 (ddd, *J* = 3, 10, 14 Hz, H-11 α , 1H), 2.21 (d, *J* = 14 Hz, H-3 α , 1H), 2.50 (ddd, *J* = 3, 12, 15 Hz, H-10 α , 1H), 4.06 (s, H-2, 1H), 4.79 (s, H-5, 1H); ¹³C NMR (125.7 MHz, CDCl₃) δ 22.51 (C-16), 23.57 (C-20), 25.22 (C-19), 25.48 (C-13), 31.57 (C-11), 31.98 (C-15), 32.76 (C-17), 32.81 (C-18), 38.81 (C-10), 40.00 (C-14), 42.23 (C-9), 42.70 (C-12), 45.91 (C-6), 47.31 (C-3), 51.67 (C-4), 62.36 (C-5), 64.44 (C-1), 75.16 (C-8), 77.77 (C-2), 99.01 (C-7). A sample for microanalysis was prepared by recrystallization from EtOH: mp 116 °C dec. Anal. Calcd for C₂₀H₃₁IO: C, 57.97; H, 7.54; I, 30.63. Found: C, 58.05; H, 7.55; I, 30.65.

Acetylation of 15. A solution of ketol **15** (0.114 g) in isopropenyl acetate (1.5 mL) was treated with *p*-toluenesulfonic acid monohydrate (0.002 g) at room temperature for 17 h. The mixture was dissolved in ether (20 mL) and washed with NaOH (2 M, 5 mL) followed by water (5 mL). The

combined aqueous fractions were re-extracted with ether (2 \times 10 mL). The combined ethereal portions were dried over anhydrous MgSO₄ and evaporated. Chromatography of the crude mixture (0.131 g) on silica (10 g), eluting with CHCl₃ gave 5 α -acetoxy-1 β *H*-laurenan-5-one (**16**) {[1*R*-(1 α ,2 $\alpha\beta$,4 $\alpha\alpha$,6 $\alpha\beta$,10 β ,10 $\alpha\beta$,10 βR^*)]-dodecahydro-1-acetoxy-2 α ,4,4,6 α ,10-pentamethylpentaleno[1,6-*cd*]azulen-3(1*H*)-one} (0.085 g, 66%): IR (film) 1736, 1242 (OAc), 1723 (C=O) cm⁻¹; ¹H NMR (500 MHz, CDCl₃) δ 0.86 (d, *J* = 7 Hz, H-16, 3H), 1.08 (s, H-17, 3H), 1.10 (s, H-19, 3H), 1.18 (m, H-14, 1H), 1.20 (s, H-20, 3H), 1.29 (s, H-18, 3H), 1.42 (m, H-12, 1H), 1.44 (m, H-10, 1H), 1.58 (m, H-13, 2H), 1.59 (dd, *J* = 4, 14 Hz, H-3, 1H), 1.60 (m, H-12, 1H), 1.82 (m, H-11, 1H), 1.83 (m, H-10, 1H), 1.84 (m, H-14, 1H), 1.88 (s, OAc, 3H), 2.00 (m, H-15, 1H), 2.05 (dd, *J* = 5, 11 Hz, H-1, 1H), 2.08 (m, H-11, 1H), 2.30 (d, *J* = 14 Hz, H-3, 1H), 2.76 (dd, *J* = 4, 12 Hz, H-7, 1H), 4.94 (dd, *J* = 4, 4 Hz, H-2, 1H); ¹³C NMR (125.7 MHz, CDCl₃) δ 21.51 (OAc), 21.95 (C-16), 22.51 (C-17), 22.81 (C-13), 22.87 (C-20), 25.09 (C-11), 27.31 (C-19), 29.47 (C-15), 29.47 (C-18), 38.59 (C-14), 40.84 (C-10), 43.77 (C-3), 47.17 (C-6), 48.18 (C-12), 49.79 (C-9), 51.01 (C-7), 51.53 (C-1), 62.11 (C-4), 65.44 (C-8), 76.36 (C-2), 170.48 (OAc), 230.13 (C-5). A sample for microanalysis was prepared by preparative TLC on silica (ether/CHCl₃ 1:19) followed by sublimation at 80 °C/5 \times 10⁻⁴ mmHg: mp 89–90 °C. Anal. Calcd for C₂₂H₃₄O₃: C, 76.26; H, 9.89. Found: C, 76.51; H, 10.01.

Acknowledgment. I thank Mervyn Thomas for NMR assistance, Nigel Perry and Dave Larsen for helpful discussions, and Mrs. M. Dick of the Campbell Microanalytical Laboratory, University of Otago, New Zealand, for microanalyses.

Supporting Information Available: NMR correlation data tables for compounds **3**, **6–9**, **11**, **13**, **14**, **16**, and **17**. This material is available free of charge via the Internet at <http://pubs.acs.org>.

JO0157340